Wetting Properties at the Submicrometer Scale: A Scanning Polarization Force Microscopy Study

F. Rieutord[†] and M. Salmeron*

Materials Sciences Division, Lawrence Berkeley National Laboratory, University of California, Berkeley, California 94720

Received: November 11, 1997; In Final Form: March 10, 1998

Submicrometer size droplets of sulfuric acid on mica have been imaged using scanning polarization force microscopy (SPFM). Our study shows that, contrary to the macroscopic case, the drop profile depends on the size of the drops, with a decrease of the contact angle with decreasing size droplets in the present case. This dependence can be explained by taking into account long-range forces between the substrate and the fluid, which prove to have important effects for submicrometer size drops. Profile measurements at the submicron scale allow direct estimation of the interaction potential between a fluid and a substrate.

Introduction

Scanning probe microscopies (SPM) have now become standard tools for the characterization of the morphology of surfaces with resolutions as fine as the atomic level. Among the different SPM techniques, the use of atomic force microscopy (AFM) does not depend on whether the sample is conductive and has consequently become very popular. There are few surfaces that have not been investigated using this technique. Fluid surfaces or surfaces of soft materials, however, are an important class of surfaces that have not yet received much investigation with these techniques. This is due to the fact that, in standard atomic force microscopy (contact mode), although the force is small ($F \sim 1$ nN), it is exerted over a tiny area ($S \sim 1$ nm^2) (that defines the lateral resolution) and produces large pressures (typically $P \sim 1$ GPa) that can easily deform the surface. In addition, there is the possibility of the liquid wetting the tip and forming a capillary neck.

New techniques have been developed to overcome this problem. One possibility is to reduce the contact time between the tip and the surface in the so-called tapping mode of operation of AFMs; this was used recently to image droplets of dendrimers, but according to the authors,[1] it is restricted to fluids showing slow molecular relaxation times and produces appreciable deformations of the surfaces under study.

Here we have used scanning polarization force microscopy (SPFM), which is a true noncontact mode of operation of the AFM, and does not suffer from these limitations. In SPFM, we make use of the attractive part of the interaction force between the tip and the surface. To enhance and better control the attractive force, an electric field is applied between the tip and the surface through biasing of the tip. Description of the first uses of this technique on liquids can be found elsewhere.[2,3] A recent review has also been recently published.[4] The smaller perturbation is at the expense of lateral resolution, which is on the order of the tip−sample distance or tip radius, i.e., typically 20−40 nm, as measured on "sharp" features such as atomic steps, depending on the tip and imaging conditions. The vertical resolution remains excellent (0.1 nm).

Wetting and spreading properties of a fluid on a smooth solid surface have often been described on a macroscopic scale using a continuum picture. Although the standard capillarity ingredients play a role, it was realized from the work of de Gennes and co-workers[5−13] that more microscopic quantities such as bulk van der Waals interactions and other long-range forces are also important, for example, in the dynamics of spreading. However, testing these predictions is a difficult task because the effects of these long-range forces are rather indirect on the macroscopic properties and, on the microscopic scale, few techniques are available to probe materials. Ellipsometry[9,13−16] and X-ray reflectivity[13] have been used but each lack lateral resolution, which is limited by the size of the probing beam (a fraction of a millimeter). The possibility of using SPM techniques with high resolution for wetting problems thus opens up an important perspective in the experimental testing of wetting theories. It should also allow one to address or avoid problems associated with substrate heterogeneities as it is easier to obtain "ideal" surfaces or ideal "defects" at micrometer sizes.

Understanding wetting at small scales has many practical applications, in particular, in relation to drop formation in atmospheric-related phenomena, spreading, and corrosion. Here we report on the observation of small droplets of sulfuric acid on freshly cleaved mica using SPFM.

Experimental Section

Materials. The experiments were conducted using a home-built AFM driven by commercial electronics[17] and enclosed in a drybox with nitrogen flow. The cantilevers used were commercial Si_3N_4 cantilevers[18] with a spring constant of 0.06 N/m. These levers were coated with 10 nm platinum film on a 5 nm titanium intermediate layer to enhance coating adhesion.

Preparation. Droplets were made in the following manner. A macroscopic drop was first deposited on the mica and then absorbed from an edge using filter paper. This leaves a surface that appears dry to the naked eye but displays an array of small droplets with various radii when scanned with a microscope. Pure sulfuric acid has a very low vapor pressure at ambient

[†] Permanent address: Département de Recherches Fondamentales sur la Matière Condensée, SI3M, Commissariat à l'Energie Atomique (CEA), 17 rue des Martyrs, 38054 Grenoble Cedex 9, France.

* Corresponding author. E-mail: salmeron@stm.lbl.gov.

S1089-5647(98)00149-7 CCC: $15.00
Published on Web 04/28/1998

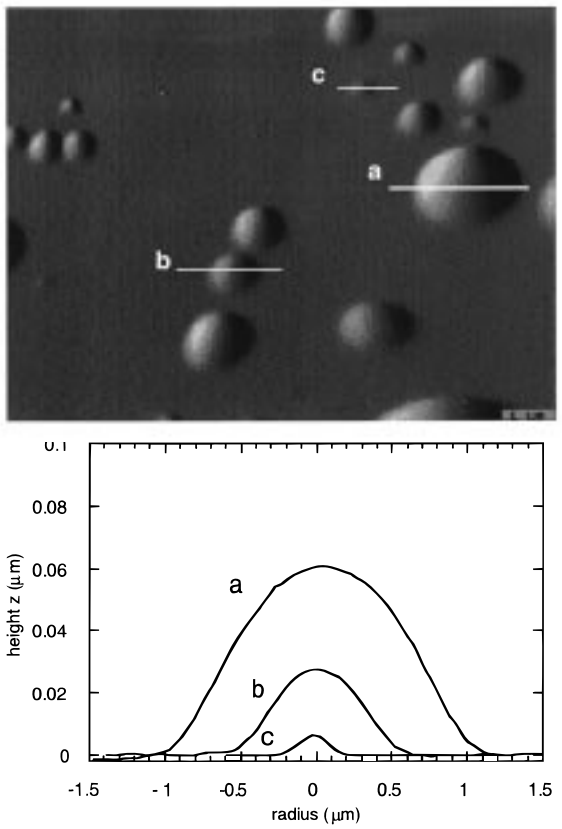

Figure 1. (a) SPFM image of sulfuric acid droplets in a drybox taken in noncontact mode (voltage = +2.5 V, spring constant of the lever k = 0.06 N/m). (b) Diameter cross sections of drops a, b, and c.

temperature, and no drop evaporation was observed during the experiments.

Results

A typical image obtained is found in Figure 1a, which shows droplets on a flat surface. The contact line around the drops is smooth and circular, revealing that no pinning occurs. Between the drops, the area is flat. Mica surfaces are known to be atomically flat over large distances so the absence of defects is not surprising. No changes in the images could be seen over time periods longer than 10 h.

In Figure 1b we show diameter cross sections of a few drops. It is seen that, for big droplets (with radius > ∼1 μm), the drop profile is essentially that of a spherical cap but with deviations close to the contact line. For smaller drops, these deviations affect the whole profile, which then appears to have a more "Lorentzian" shape, with an inverted curvature close to the contact line.

For these small drops, the notion of "contact angle" or "contact line" per se is meaningless as the whole profile changes, and there is no slope discontinuity in the contact region. Still, "contact angle" is a useful parameter to compare the small and large size cases and model the profile dependence with the size of the drops. Here we shall adopt as a definition for "contact angle" the maximum value of the slope along a diametrical cross section, i.e., the angle at the inflection point on the drop profile. In a similar way, the radius of the drop (in the surface plane) will be defined as the radial coordinate of this point.

When plotted as a function of drop size (Figure 2), the contact angle decreases with increasing drop radius and starts to deviate from its macroscopic value for radii < 1 μm and going to zero for $r = 0$.

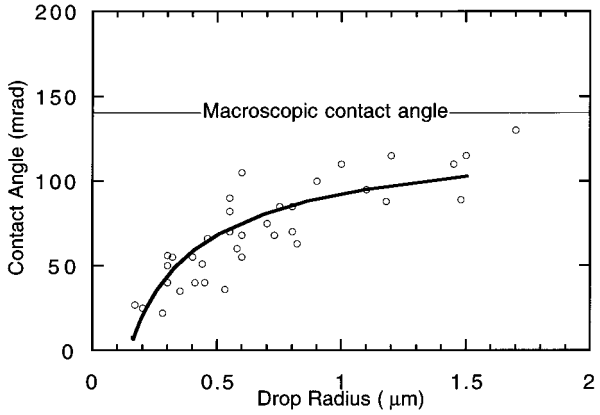

Figure 2. Contact angle as a function of drop radius. The solid line is the calculation using the model described in the text.

Experiments also show that the area between the drops is not bare mica but is covered by a liquid film of a few layers thickness. Direct measurement of the thickness of the film in the flat part is difficult with our technique since the film is perfect and there are few defects on the mica. The presence of this film can be shown only through force−distance curves which show larger hysteresis between approach and retraction than on bare mica.

The observation of drops of a liquid on top of a film of the same substance is often referred to as "pseudopartial"[7] or "autophobic" wetting. Observation of such wetting behavior on mica substrate can be expected in our case due to the large surface energy of cleaved mica. Values of 300−600 mJ/m^2 have been reported for the surface energy of freshly cleaved mica,[1] compared with 53 mJ/m^2 for the surface tension of sulfuric acid. The large polarizability of sulfuric acid (dielectric constant $\epsilon = 95$) yields a positive Hamaker constant ($A > 0$) using the standard definition[8] of Hamaker constants. Note that in refs 5−7 the sign convention is opposite.

An optical determination of the macroscopic contact angle was made using a commercial Ramé-Hart contact angle goniometer. The value found (8 ± 1°) is also shown in Figure 2.

Discussion

Effect of Finite Resolution on the Drop Profile Measurements. The profile recorded is a convolution of the true profile by the instrumental resolution. This instrumental resolution in SPFM is due to the tip radius and to the nonzero distance between the tip and the surface. Both distances are of the same order of magnitude, 20−40 nm.

The reduction in height associated with the tip moving at a distance d from the surface can be estimated using the exactly solvable model of a point charge above a half-sphere protruding from a plane.[19] In this model, the interaction between the charge borne by the polarized tip and the surface can be described using a four-charge model (the tip charge and three image charges). This simple model shows that the maximum variation in the tip−surface distance necessary to keep the force constant does not exceed 15%, whatever the relative values of the tip−surface distance and sphere radii. In our case (see Figure 1b), the drops are rather flat lenses so this effect is expected to be much smaller (0.01% for the smallest drop). The resulting effect on the contact angle/change of profile is negligible.

As mentioned above, in the experiments investigating the flattening of the drop profile by finite lateral resolution, the lateral resolution is better than 60 nm fwhm (tip radius). The smallest drop of Figure 1b has a radius (fwhm) of ∼220 nm.

The convolution of such a profile by the given resolution results in an underestimation of ~4% on the slope of the profile. We have not corrected for this small effect.

Effect of Change of Dielectric Constant across the Surface. In SPFM, the force between the charged tip and the sample depends mainly on two parameters: the distance to the surface and the dielectric constant of the material on the surface. Therefore, in principle, the image obtained by maintaining F constant reflects changes in both true topography and dielectric constants. In our case, the dielectric constant of the material under the tip is not constant due to two effects: (1) our system involves two materials, one of which is the liquid film of variable thickness, and (2) in very thin films, we can expect a reduction of the mobility (the polarizability) of the liquid in the field of the substrate.

We have estimated these two effects using the image charge description[3] of the interaction between a point charge and a dielectric film (dielectric constant ϵ_1) on a dielectric material (dielectric constant ϵ_2):

$$F = \frac{1}{4\pi\epsilon_0}\frac{\gamma_1 q^2}{(2z)^2}(1+\xi) \tag{1}$$

with

$$\xi = \frac{{\gamma_1}^2 - 1}{\gamma_1}\sum_{i\geq 0}\frac{{\gamma_1}^i{\gamma_2}^{i+1}}{(1+(i+1)L/z)^2}$$

where $\gamma_1 = (\epsilon_1 - 1)/(\epsilon_1 + 1)$ and $\gamma_2 = (\epsilon_1 - \epsilon_2)/(\epsilon_1 + \epsilon_2)$, z is the tip−surface distance, and L is the thickness of the liquid on the substrate. We have calculated the error term ξ as a function of the ratio L/z and the dielectric constant ϵ_1. For values of ϵ_1 ranging between 7 (the dielectric constant of mica, ϵ_2) and 95 (the dielectric constant of free [bulk] sulfuric acid), these calculations show that variations of this term never exceeds 10% for the relevant set of values L/z and ϵ_1. So even if the polarizability of sulfuric acid were strongly reduced in the thin film where it may have a solidlike structure, the effect would be small (maximum error of 1 nm). It should be noted that, in our case, changes of dielectric constant across the surface would overestimate the contact angle of small drops since mica has a smaller dielectric constant than sulfuric acid.

Perturbation of the Drop Shape by the Tip. As mentioned in the Introduction, this effect is a limitation of the AFM technique in the investigation of soft materials and has to be carefully addressed. In the case of small drops, the relevant parameter for estimating the perturbation is the ratio of the pressure exerted by the tip $P = F/S$ to the Laplace pressure $P_L = 2\gamma/r$. This ratio has to be kept as small as possible. We can achieve this in our case since F is small (soft lever and small voltage leads to $F < 0.05$ nN), S is large (~1000 nm^2), and r is small (<1 μm).

Note that it is possible to observe the effects of the tip on the drop in SPFM. Scanning at high force set point values using a stiff lever may cause the drop to distort or even move.[21] During the experiments, the images were scanned at different voltages using different force set points, i.e., different tip/surface distances, to ensure that the measured features were insensitive to the applied force.

Modeling

The decrease of contact angle as a function of droplet size obviously cannot be described using capillary arguments alone. They would predict a constant angle given by the Young relation, which does not involve the size of the drop. Thus, this effect is a direct signature of the effect of additional terms in the free energy of the system, specifically, long-range forces. We analyze our data using the theoretical model of refs 5−10.

We use the following expression for the free energy functional:

$$F(z,\dot{z},r) = \int_r ({}^1/_2\gamma\dot{z}^2 + P(z) - P(0))2\pi r\,\mathrm{d}r \tag{2}$$

where γ is the liquid−vapor surface tension, $P(z)$ describes the interaction potential between the liquid and the substrate due to long-range forces, and $z(r)$ is the drop profile. This form assumes that the contact angle $\dot{z}$ is small everywhere.

The shape of the drop is given by the minimization of this functional with the condition that its volume

$$V = \int z(r)2\pi r\,\mathrm{d}r \tag{3}$$

is constant.

The Euler−Lagrange equation of this variational problem reads

$$\ddot{z} + \dot{z}/r = -\lambda + p'(z) \tag{4}$$

where $p'(z) = \mathrm{d}p(z)/\mathrm{d}z = (1/\gamma)\mathrm{d}P(z)/\mathrm{d}z$ and λ is a Lagrange multiplier.

In the one-dimensional case,[3,5,6] the term $\dot{z}/r$ does not appear, and eq 4 has a simple first-order integral:

$${}^1/_2\dot{z}^2 = -\gamma(z - z_0) + p(z) - p(z_0) \tag{5}$$

This form can then be used to predict the shape of a drop close to the contact line, which is justified in the case of a large drop when the curvature around the vertical axis can be neglected. In our case, since our drops are small, one has to keep the full form of eq 4. In general, and with the potential $p(z)$ chosen below, the second-order nonlinear eq 4 has no simple first-order integral, due to the $\dot{z}/r$ term or to the fact that F depends on r explicitly. The solution must then be performed numerically from the second-derivative stage, with the boundary conditions $z(0) = z_0$ and $\dot{z}(0) = 0$.

In principle, eq 4 or, when applicable, its first integral (5) gives a key to a new method for determining the interaction potential $p(z)$. Since we are able to record the profile $z(r)$ (and its derivatives) accurately, we can basically use these data to determine $p'(z)$ and $p(z)$ (see below).

We performed the numerical minimization of (2) in the following way. Given a drop volume V and an expression for the potential $p(z)$, we find for each value of λ the solution $z_{\lambda,V}(r)$ of eq 4 that satisfies condition (3), i.e., find the value z_0 that yields volume V. Then we use in (2) the value of F corresponding to this set of parameters (V and λ) and minimize it over λ. The procedure was checked in the case of $p(z) = 0$ where it yielded spherical cap-shaped drops with a contact angle given by the Young equation: $\gamma\cos\theta = \gamma_{SV} - \gamma_{SL}$. In this case, $p(0)$ is equal to the spreading parameter $S = \gamma_{SV} - \gamma - \gamma_{SL}$ and is negative. We also checked the procedure against some of the predictions of ref 7, notably in the so-called "pancake case" ($S > 0$, concave potential).

To model our data, we have used a potential

$$p(z) = \frac{1}{\gamma}P(z) = -\frac{a^2}{2(z+b)^2} \tag{6}$$

Such a potential can be expected when taking into account only

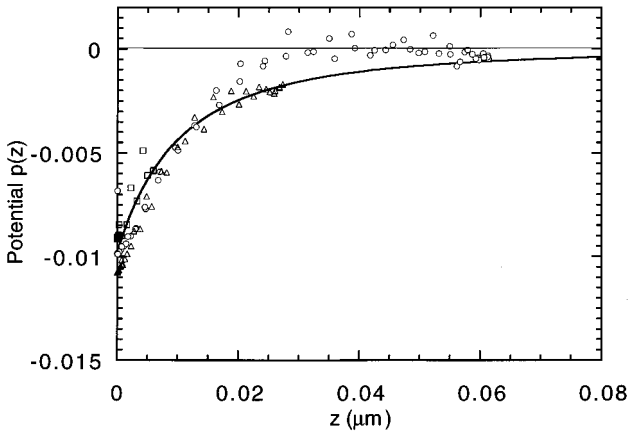

Figure 3. Potential [$p(z)$] as obtained from the direct inversion of the profiles of Figure 1b. The solid line is the potential used to account for Figure 2 data.

van der Waals forces. The constant a is a molecular length which is related to the Hamaker constant difference $A = A_{LL} - A_{SL}$ via

$$a^2 = A/6\pi\gamma \tag{7}$$

In our case, $A > 0$. The presence of the offset value b in expression 6 was used to account for the partial wetting behavior of the liquid, allowing z to be referenced to the surface of the film.

The value $p(0) = -a^2/2b^2$ thus acts as an effective (negative) spreading parameter for the liquid on top of its own film, and its value determines the macroscopic contact angle θ_0 through $\theta_0^2/2 = -p(0)$.

We performed two types of analysis of the image data. In the first one (Figure 2), we extracted only one characteristic parameter per drop profile, the contact angle, for different drops on several images. We then calculated the profiles for different volumes of drops using the above formalism and the theoretical contact angle vs drop size. Fitting this to experimental data gives a value of $a = 2.8$ nm.

In the second type of analysis (Figure 3), we perform a direct inversion of the experimental profiles of Figure 1b using eq 4, taking for λ the value obtained for a drop of the same volume. The potential obtained is consistent with the description used to account for the contact angle measurements. This shows that drop profile measurements with SPFM can be used as an effective tool to measure interaction potentials.

In the case of sulfuric acid, although it is a highly polarizable material, it is likely that van der Waals forces are not the only forces at play, and thus the value for a should be taken only as a parameter in the description of the interaction potential using the form of eq 6. A small amount of water may also be present in sulfuric acid with associated electrostatic forces that may also enter the experimentally determined interaction potential.

Conclusion

The possibility of imaging droplets at a submicroscopic scale by SPFM opens up a wide perspective in the experimental study of wetting, since the resolution of the method allows one to study systems whose sizes are in the range of most intermolecular forces. This possibility may benefit many practical problems. For example, film buildup from droplet deposition is a technique commonly used in industry. Also, with the ability to control and image the surface at the atomic level, we are less subject to substrate heterogeneity problems than with macroscopic measurements. Note, furthermore, that this technique is not restricted to nonwetting cases. We recently performed experiments on the spreading of a lubricant on graphite substrate. The spreading coefficient was positive, but spreading was limited by repulsive interaction between the two interfaces. The profile of the so-called "pancake"-shaped drop could be inverted in a similar way to obtain the interaction profile $p(z)$.[22]

Finally, it should be mentioned that the problem of contact angle dependence on drop size was previously addressed for macroscopic drops (millimeter size), using the concept of line tension (σ) and a modified Young equation.[23] Measurements of such a line tension have been done with a wide range of results. Theoretical calculations by Joanny and de Gennes[10] have shown that line tension can be derived from the effects of long-range forces. They have predicted values for σ on the order of γa, a being the molecular length defined above for van der Waals forces. For such a small value of σ, the effect on drop shapes should be visible on microscopic drops only. The observation of values several orders of magnitude larger (with effects on millimeter size drops) should probably be attributed to microscopic heterogeneity of the substrate at the contact line.

Acknowledgment. Discussions with Drs. H. Bluhm, R. W. Carpick, M. Enachescu, D. F. Ogletree, and L. Xu are gratefully acknowledged. We thank D. A. Schleef for his help in the computations and reading the manuscript. F.R. acknowledges a grant from NATO. This work was supported by the Lawrence Berkeley National Laboratory through the Director, Office of Energy Research, Basic Energy Science, Materials Science Division of the U.S. Department of Energy, under Contract No. DE-AC03-76SF00098.

References and Notes

(1) Sheiko, S.; Muzafarov, A.; Winkler, R.; Getmanova, E.; Eckert, G.; Reinecker, P. *Langmuir* **1997**, *13*, 4172.
(2) Mate, C. M.; Lorenz M. R.; Novotny V. J. *J. Chem. Phys.* **1989**, *90*, 7550.
(3) Hu, J.; Xiao, X. D.; Salmeron, M. *Appl. Phys. Lett.* **1995**, *67*, 476.
(4) Salmeron, M.; Xu, L.; Hu, J.; Dai, Q. *MRS Bull.* **1997**, *22*, 36.
(5) Joanny, J. F.; de Gennes, P. G. *C. R. Acad. Sci. Paris, Ser. II* **1984**, *299*, 605.
(6) de Gennes, P. G. *Rev. Mod. Phys.* **1985**, *57*, 827.
(7) Brochard, F.; di Meglio, J. M.; Quéré D.; de Gennes, P. G. *Langmuir* **1991**, *7*, 335.
(8) Israelachvili, J. *Intermolecular and Surface Forces*; Academic Press: New York, 1985.
(9) Joanny, J. F.; de Gennes, P. G. *C. R. Acad. Sci. Paris, Ser. II* **1986**, *5*, 337.
(10) Joanny, J. F.; de Gennes, P. G. *J. Colloid Interface Sci.* **1986**, *111*, 94.
(11) Cazabat, A. M. In *Liquids at Interfaces;* Charvolin, J., Joanny, J. F., Zinn-Justin, J., Eds.; North-Holland: New York, 1990.
(12) Léger, L.; Joanny, J. F. *Rep. Prog. Phys.* **1992**, 431.
(13) Daillant, J.; Benattar J. J.; Bosio, L.; Léger, L. *Europhys. Lett.* **1988**, *6*, 431.
(14) Heslot, F.; Fraysse, N.; Cazabat, A. M. *Nature* **1989**, *338*, 640.
(15) Valignat, M. P.; Fraysse, N.; Cazabat, A. M.; Heslot, F.; Levinson, P. *Thin Solid Films* **1993**, *234*, 475.
(16) Villette, S.; Valignat, M. P.; Cazabat, A. M.; Schabert, F. A.; Kalachev, A. *Physica A* **1997**, *236*, 123.
(17) STM 100 electronics, RHK Technology, Rochester Hills, MI.
(18) Digital Instruments, Santa Barbara, CA.
(19) Durand, E. *Electrostatique et Magnetostatique*; Masson: Paris, 1953.
(20) Hall, D. G.; Cole, R. H. *J. Phys. Chem.* **1981**, *85*, 1065.
(21) Hu, J.; Carpick, R. W.; Salmeron, M. *J. Vac. Sci. Technol. B* **1996**, *14*, 1341.
(22) Xu, L.; Artsyukhovich, A.; Rieutord, F.; Salmeron, M. Manuscript in preparation.
(23) Gaydos, J.; Neumann, A. W. *J. Colloid Interface Sci.* **1987**, *120*, 76.